Atmospheric and Oceanic Science Letters 15 (2022) 100189

Contents lists available at ScienceDirect

Atmospheric and Oceanic Science Letters

journal homepage: http://www.keaipublishing.com/en/journals/atmospheric-and-oceanic-science-letters/

Impacts of ENSO on wintertime $PM_{2.5}$ pollution over China during 2014–2021

Biyin Xie, Yang Yang*, Pinya Wang, Hong Liao

Jiangsu Key Laboratory of Atmospheric Environment Monitoring and Pollution Control, Jiangsu Collaborative Innovation Center of Atmospheric Environment and Equipment Technology, School of Environmental Science and Engineering, Nanjing University of Information Science and Technology, Nanjing, China

A R T I C L E I N F O

Keywords:
$PM_{2.5}$
ENSO
atmospheric circulation
precipitation
关键词:
$PM_{2.5}$
厄尔尼诺–南方涛动
大气环流
降水

A B S T R A C T

China has implemented a series of emission reduction policies since 2013, and the concentration of air pollutants has consequently decreased significantly. However, $PM_{2.5}$ (particulate matter with an aerodynamic diameter less than 2.5 μm) pollution still occurs in China in relation to the interannual variations in meteorological conditions. Considering that El Niño–Southern Oscillation (ENSO) is the strongest signal modulating the interannual variation in the atmosphere–ocean system, in this study the authors investigate the variations in $PM_{2.5}$ concentrations in four megacity clusters of China during the winter season associated with four individual ENSO events from 2014 to 2021. Results show that the wintertime $PM_{2.5}$ concentrations in the Beijing–Tianjin–Hebei and Fenwei Plain regions during El Niño years are higher than those during La Niña years, which can be explained by the anomalous southerly (northerly) winds during El Niño (La Niña) favoring $PM_{2.5}$ accumulation (diffusion). In the Pearl River Delta region, $PM_{2.5}$ concentrations decrease in El Niño relative to La Niña years owing to the enhanced water vapor flux and precipitation, removing more $PM_{2.5}$ from the atmosphere. The comprehensive effects of wind and precipitation anomalies lead to the unpredictability of the impacts of ENSO on $PM_{2.5}$ over the Yangtze River Delta region, which should be analyzed case by case.

摘要

2013年以来中国实施了一系列减排政策, 大气污染物浓度明显下降, 但由于气象条件的年际变化, 中国$PM_{2.5}$ (空气动力学直径小于2.5 μm的颗粒物) 污染仍然存在. 厄尔尼诺–南方涛动 (ENSO) 是调节大气–海洋系统年际变化的最强信号. 本文研究了2014–2021年四次ENSO事件期间, 中国四个特大城市群冬季$PM_{2.5}$浓度的变化. 结果表明, 在京津冀和汾渭平原地区, 由于厄尔尼诺 (拉尼娜) 期间的偏南风 (偏北风) 异常有利于 $PM_{2.5}$ 的积累 (扩散), 冬季$PM_{2.5}$浓度在厄尔尼诺年高于拉尼娜年. 在珠三角地区, 由于厄尔尼诺冬季水汽通量和降水的增加有利于大气中$PM_{2.5}$的湿清除, 冬季$PM_{2.5}$浓度在厄尔尼诺年低于拉尼娜年. 在环流和降水异常的综合作用下, ENSO对长三角地区$PM_{2.5}$浓度的影响难以预测, 应逐案分析.

1. Introduction

$PM_{2.5}$ refers to particulate matter with an aerodynamic diameter less than 2.5 μm. It can stay in the air for several days and be transported over long distances, posing serious impacts on public health and socioeconomics. China has experienced frequent severe $PM_{2.5}$ pollution since the beginning of the 21st century. For instance, $PM_{2.5}$ pollution was reported to be responsible for more than one million premature deaths in China during the year 2015 (Cohen et al., 2017).

The rise of anthropogenic emissions and adverse meteorological conditions are the main factors leading to increases in regional $PM_{2.5}$ concentrations in recent years (Ding et al., 2016; Ding and Liu, 2014; Yang et al., 2016, 2018). The frequency of severe winter haze events in Beijing in the future (2050–2099) is projected to increase by 50% compared to historical periods (1950–1999), as global greenhouse gas emissions accelerate the warming of the lower atmosphere and weaken the East Asian winter monsoon (Cai et al., 2017). In addition, external forcing, such as El Niño–Southern Oscillation (ENSO), Pacific Decadal Oscillation (PDO), and Arctic sea ice also have important impacts on $PM_{2.5}$ pollution in China (e.g., Chang et al., 2016; Yin et al., 2021). Arctic sea ice loss intensifies the haze pollution in eastern China (Wang et al., 2015; Zou et al., 2020). With PDO shifting towards a negative phase, the weakened Mongolian high and ascending motion anomalies destabilize the air, which is conducive to the spread of pollutants and has led to the decline in the occurrence of wintertime haze over central-eastern China since the mid-1980s (Zhao et al., 2016).

Among the external forcings, ENSO is the strongest signal that modulates interannual variations in the ocean–atmosphere system near the

* Corresponding author.
E-mail address: yang.yang@nuist.edu.cn (Y. Yang).

https://doi.org/10.1016/j.aosl.2022.100189
Received 13 December 2021; Revised 5 January 2022; Accepted 20 January 2022
Available online 11 February 2022

equator. ENSO oscillates irregularly between its warm (El Niño) and cold (La Niña) phases, peaking in the boreal winter and recurring in two to seven years. It triggers atmospheric circulation and precipitation anomalies, thereby affecting the chemical formation, transport, and removal of air pollutants. For example, Liu et al. (2019) quantified the covariability between 1948–2015 observed East China precipitation and tropical Pacific SST and reported that Southeast China wintertime flooding (drought) was related to tropical Pacific El Niño (La Niña) SST. Previous studies have investigated the influences of ENSO on air pollutants through observational records and model simulations. Based on atmospheric visibility data, Gao and Li (2015) showed that wintertime haze days in eastern China increased (decreased) in El Niño (La Niña) during 1981–2010; and again based on visibility data, Zhao et al. (2022) found that the impact of ENSO on haze pollution over northern China was strong in early winter, but weak in late winter. Using an aerosol–climate coupled model, Zhao et al. (2018) found that aerosol levels over southern China increased (decreased) in El Niño (La Niña) winter, contributed by aerosols transported from South and Southeast Asia. Based on an atmospheric circulation model, Sun et al. (2018) found that the weakened East Asian winter monsoon during El Niño events increased aerosols in eastern China, especially over northern China. Using observational data, Wang et al. (2019) found that wintertime $PM_{2.5}$ concentrations over northern (southern) China were higher (lower) in the 2015 El Niño than in the 2017 La Niña.

ENSO events characterized by different intensities, durations and patterns of equatorial SST anomalies could have different impacts on aerosol pollution in China. Based on model simulations, Yu et al. (2019) classified El Niño events into five categories with different spatial types and intensities, and revealed that Central Pacific (CP) El Niño events led to larger increases in the winter aerosol burden over southern China relative to Eastern Pacific (EP) El Niño events with the same intensity. Wang et al. (2020) found that haze days in Beijing were more frequent during EP El Niño winters and less frequent during EP La Niña winters. Zeng et al. (2021) found that, compared to long-duration El Niño events, El Niño with short duration but strong intensity caused northerly wind anomalies over central-eastern China, which was favorable for aerosol diffusion over this region. Yet, some discrepancies exist among previous works; for example, Zhao et al. (2018) and Yu et al. (2019) found that winter aerosols increased in southern China during El Niño years, but Wang et al. (2019) reached opposing conclusions.

Due to the lack of long-term observational $PM_{2.5}$ data, all previous research has been based on atmospheric visibility data, modeling simulations or limited surface measurements during individual El Niño and/or La Niña events. In 2013, the Chinese government issued the Air Pollution Prevention and Control Action Plan (hereafter, Clean Air Action) to control anthropogenic emissions and required the Beijing–Tianjin–Hebei (BTH) region, Yangtze River Delta (YRD), and Pearl River Delta (PRD) to reduce their $PM_{2.5}$ concentrations by 15%–25% from 2013 to 2017. Since then, nationwide $PM_{2.5}$ concentration data have been provided by the China National Environmental Monitoring Center (CNEMC). In 2018, the Three-year Action Plan on Blue Sky Protection Campaign (hereafter, Blue Sky Protection Campaign) was issued for continuous emissions reduction, mainly concentrating on three key regions, BTH and surrounding areas, Fenwei Plain (FWP) and YRD. Here, based on $PM_{2.5}$ observational data during 2014–2021, we quantify the variations in wintertime $PM_{2.5}$ concentrations in four megacity clusters in China, i.e., BTH, FWP, YRD, and PRD, during El Niño and La Niña years and explore the possible mechanisms of the ENSO effects on $PM_{2.5}$ in China.

2. Data and methods

To identify the ENSO conditions, we apply monthly SST data from the National Oceanic and Atmospheric Administration Extended Reconstructed SST version 5 (Huang et al., 2017). Hourly observations of $PM_{2.5}$ concentrations over China from September 2014 to August 2021 are derived from CNEMC (http://www.cnemc.cn). Sites of the $PM_{2.5}$ nationwide monitoring network increased in the past few years, with about 1000 sites in September 2014 and about 2000 sites in August 2021. We use 1439 stations of which at least 60% data records are available within the analyzed period (shown in Fig. S1). Monthly mean geopotential height, wind fields, and specific humidity data are derived from ERA5 (Hersbach et al., 2020) provided by the European Centre for Medium-Range Weather Forecasts. Monthly precipitation data are extracted from the CPC Merged Analysis of Precipitation (Xie and Arkin, 1997).

ENSO events are indicated by Niño3.4 index, which is defined as the regionally averaged SST anomaly over the Niño3.4 region (5°S–5°N, 170–120°W), shown in Fig. 1. Anomalies are calculated by removing the 1991–2020 average. When the three-month running Niño3.4 index is above 0.5°C (below −0.5°C) and lasts for more than five months, it is identified as an El Niño (La Niña) event. During an ENSO event, if the center of SST anomalies is west of 150°W, we classify the event as a CP event; otherwise, an EP event. Based on these criteria, the four strongest ENSO events during 2014–2021 are identified, which are in the winters of 2015 (El Niño), 2017 (La Niña), 2018 (El Niño), and 2020 (La Niña) (see Table 1).

Table 1 El Niño and La Niña events identified in this study over 2014–2021.

Type	Period	Length (month)	Maximum time	Maximum (°C)	Type
El Niño	2014.11–2016.04	18	2015.12	2.6	EP
La Niña	2017.10–2018.04	7	2017.12	−1.0	EP
El Niño	2018.10–2019.05	8	2018.11	0.9	CP
La Niña	2020.08–2021.04	9	2020.11	−1.3	EP

3. Results

Time series of monthly mean $PM_{2.5}$ concentrations averaged over the 1439 stations over China are shown in Fig. S2. It is obvious that the $PM_{2.5}$ concentration throughout China have declined since 2014 due to the Clean Air Action and Blue Sky Protection Campaign. In addition, the $PM_{2.5}$ concentration exhibits significant annual variability and usually reaches its peak in winter—the same season as when ENSO reaches its mature phase.

Fig. 2 presents the year-by-year changes in $PM_{2.5}$ concentrations in December–January–February (DJF) over the four sub-regions of China focused upon in this study. The seasonal and regional averaged $PM_{2.5}$ concentrations are 95 $\mu g\ m^{-3}$ in BTH, 97 $\mu g\ m^{-3}$ in FWP, 65 $\mu g\ m^{-3}$ in YRD, 40 $\mu g\ m^{-3}$ in PRD, and 64 $\mu g\ m^{-3}$ throughout the whole of China during the analyzed period. The $PM_{2.5}$ concentrations in BTH and FWP are generally higher in El Niño winters than in La Niña winters, whereas lower concentrations appear in PRD. More specifically, compared with winter 2017 (2020), the $PM_{2.5}$ concentration in BTH and FWP in winter 2015 (2018) increased by 27 (29) $\mu g\ m^{-3}$ and 2 (37) $\mu g\ m^{-3}$, respectively. Even if anthropogenic emissions were declining with time, the $PM_{2.5}$ concentrations over BTH and FWP during the 2018 El Niño were 11 $\mu g\ m^{-3}$ and 9 $\mu g\ m^{-3}$ higher than those during the 2017 La Niña, suggesting that ENSO's modulation of $PM_{2.5}$ concentrations could be stronger than anthropogenic emissions on interannual timescales. The $PM_{2.5}$ concentrations over PRD in the 2015 (2018) El Niño winter were 16 $\mu g\ m^{-3}$ (1 $\mu g\ m^{-3}$) lower than those in the 2017 (2020) La Niña. In YRD, the $PM_{2.5}$ concentrations in the 2015 (2018) El Niño were 3 $\mu g\ m^{-3}$ (10 $\mu g\ m^{-3}$) higher than those in the winter 2017 (2020) La Niña, but the concentration in 2018 was 12 $\mu g\ m^{-3}$ lower than that in 2017.

Fig. 3 shows the spatial patterns of DJF-mean $PM_{2.5}$ concentrations during the four ENSO events over China, as well as differences between El Niño and La Niña years. The $PM_{2.5}$ concentrations in the four winters have a similar spatial pattern, with higher $PM_{2.5}$ concentrations in eastern China, especially in BTH, but lower concentrations in western

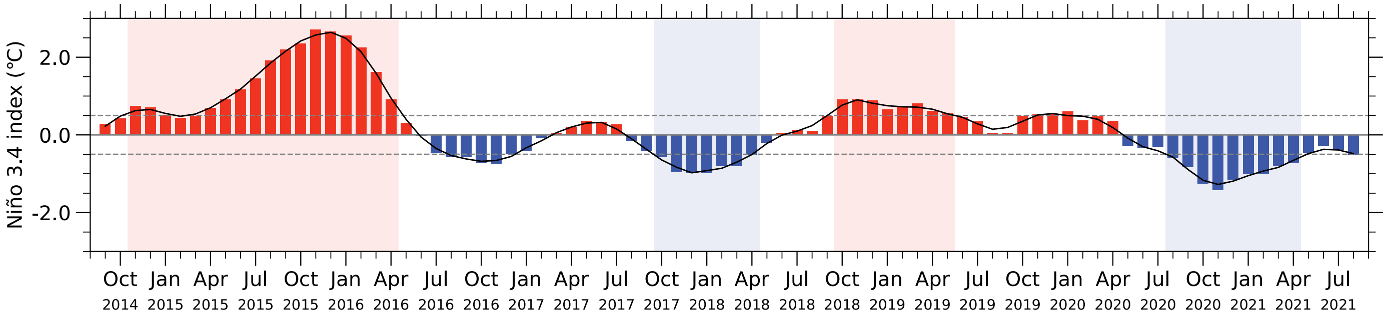

Fig. 1. Time series of Niño3.4 index (bars; units: °C) and its three-month running mean (curve; units: °C). Shades illustrate El Niño (red) and La Niña (blue) periods. Dotted lines indicate 0.5°C and −0.5°C.

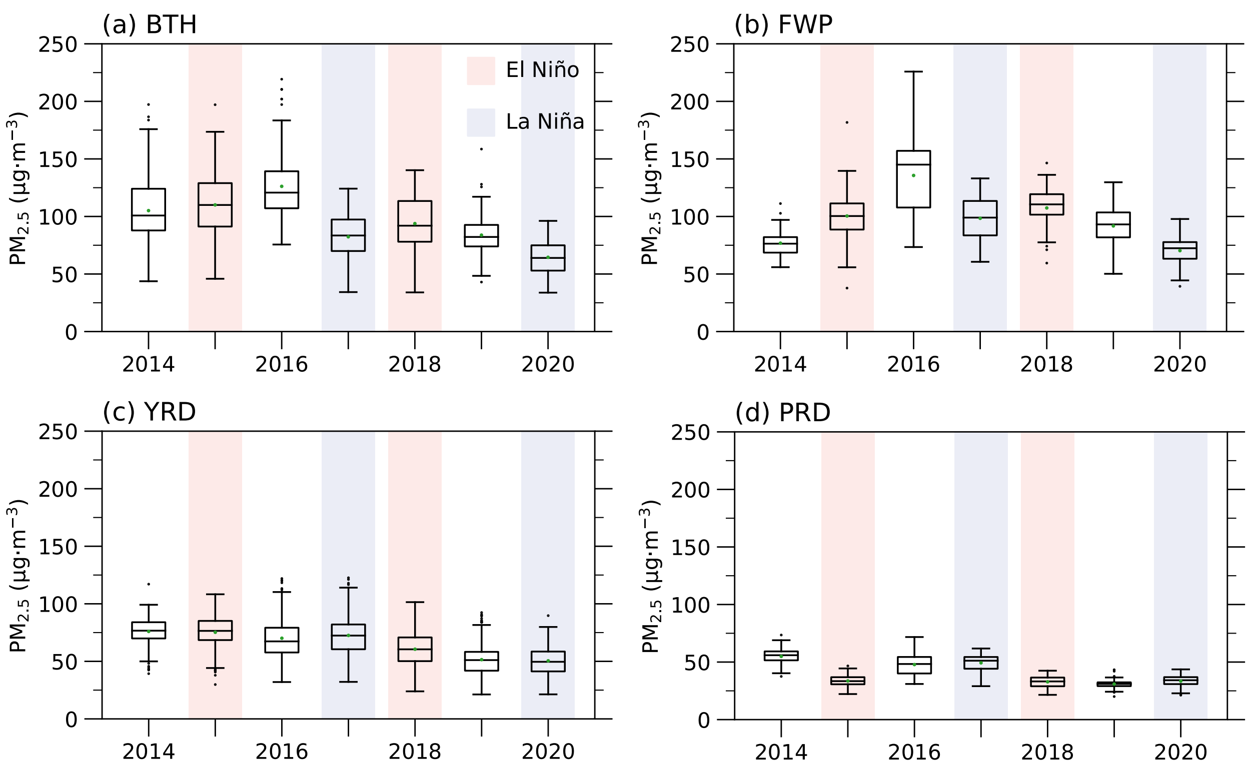

Fig. 2. $PM_{2.5}$ concentrations (units: $\mu g\ m^{-3}$) in winter (DJF) in the BTH, FWP, YRD, and PRD regions of China. The boxes denote the first and third quartiles of the data; the horizontal lines indicate the median; and the green points indicate the mean. The whiskers extend from the boxes by 1.5 times the interquartile range. Shades illustrate El Niño (red) and La Niña (blue) years.

and southern China. Moreover, by comparing the $PM_{2.5}$ concentrations between El Niño and La Niña winters, obvious differences exist between northern and southern China. The DJF $PM_{2.5}$ concentrations show positive anomalies in northern China during El Niño events (2015 and 2018) relative to La Niña events (2017 and 2020) (Fig. 3(e, g)). Considering the emission reductions in recent years, we compare the winter $PM_{2.5}$ concentrations between 2017 and 2018 (Fig. 3(f)), and the difference shows the same pattern as above. The differences exhibit a maximum of more than 50 $\mu g\ m^{-3}$ over northern China. In the area south of the Yangtze River, the differences are generally the opposite, with lower concentrations in El Niño than in La Niña winters.

To explore underlying mechanisms associated with ENSO influences on wintertime $PM_{2.5}$ concentrations in China, we analyze the DJF-mean large-scale atmospheric circulation anomalies, including geopotential height, wind fields, and precipitation, relative to the 42-year climatology (seasonal means averaged over 1979–2020), as shown in Fig. 4.

During the 2015 and 2018 El Niño, the western North Pacific subtropical high and the Aleutian low strengthened significantly, leading to anomalous southeasterly winds in the lower atmosphere over BTH and FWP relative to the climatological mean, which was not conducive to the diffusion of air pollutants. Although anomalous southeasterly winds at 850 hPa were apparent over BTH and FWP in December 2015, they reversed to anomalous northerlies in January and February 2016 (Fig. S3), which was due to the beginning of the decay of El Niño and the sudden phase change of the Arctic Oscillation from positive to negative (Zhang et al., 2019). During the 2017 and 2020 La Niña, the Aleutian low shifted westward, leading to anomalous low pressure over Northeast China. In winter 2017, the northerly winds at 850 hPa over BTH and FWP were strengthened, which contributed to the diffusion of $PM_{2.5}$ and thereby decreased the $PM_{2.5}$ concentrations over BTH and FWP and increased them over YRD owing to the regional transport from northern China. In winter 2020, the anomalous westerly winds at 850 hPa and southwesterly wind at 500 hPa that existed over BTH and FWP were also favorable for $PM_{2.5}$ diffusion.

$PM_{2.5}$ over southern China is largely influenced by the precipitation associated with the moisture transport from the oceans. Fig. S4

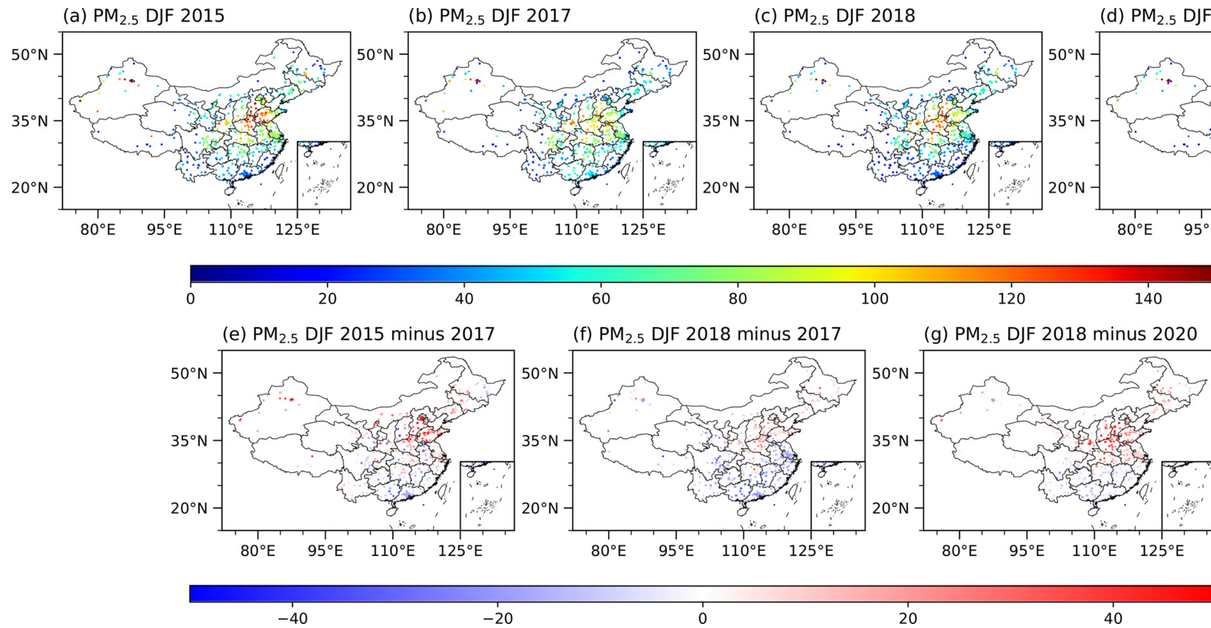

Fig. 3. Spatial distribution of $PM_{2.5}$ concentration (units: $\mu g\ m^{-3}$) in DJF during the (a) 2015 El Niño, (b) 2017 La Niña, (c) 2018 El Niño, and (d) 2020 La Niña, and the differences in $PM_{2.5}$ concentrations (e) between the 2015 El Niño and 2017 La Niña, (f) between the 2018 El Niño and 2017 La Niña, and (g) between the 2018 El Niño and 2020 La Niña.

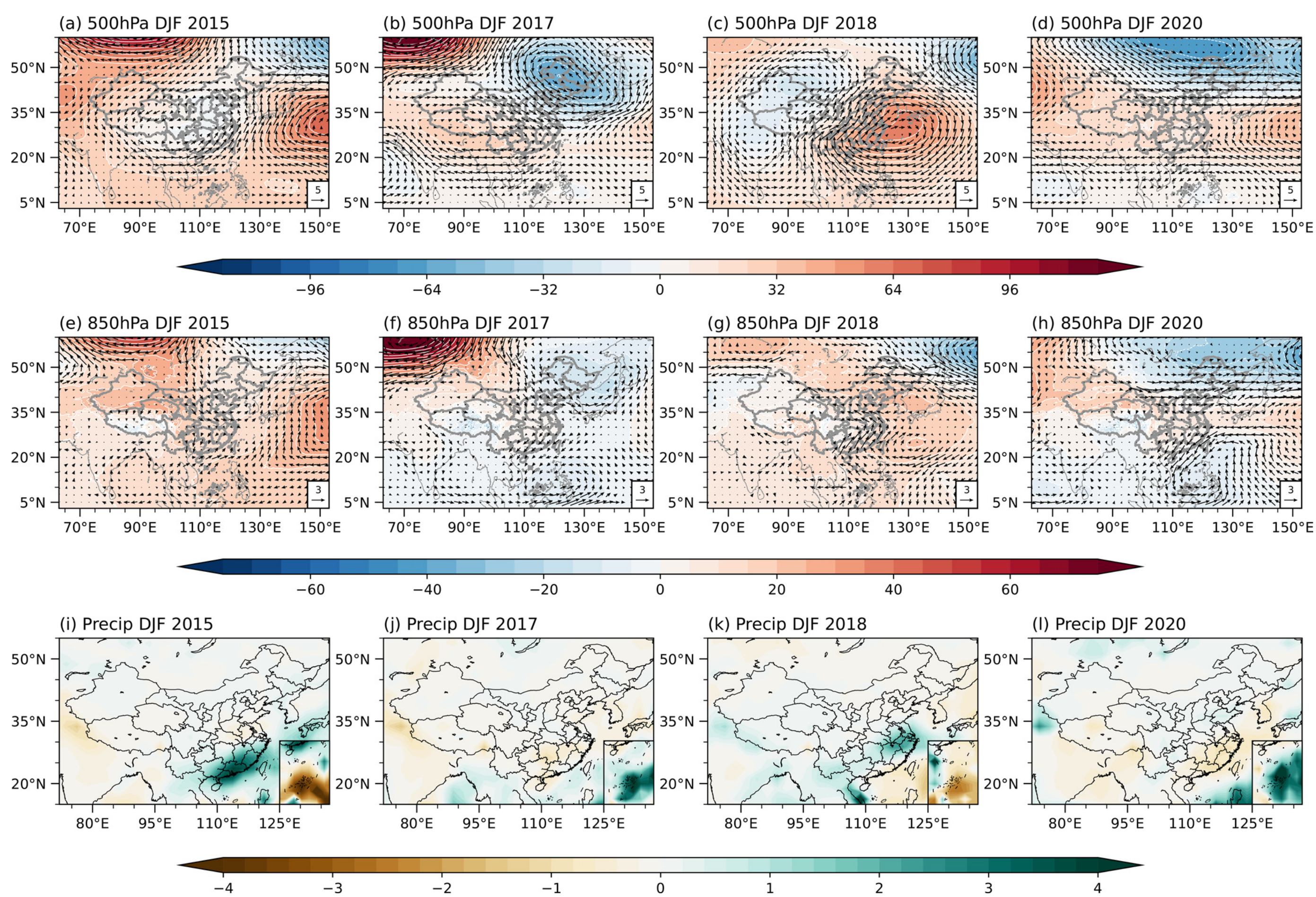

Fig. 4. Geopotential height (units: gpm) and wind (units: $m\ s^{-1}$) anomalies at (a–d) 500 hPa and (e–h) 850 hPa, and (i–l) precipitation (units: $mm\ d^{-1}$) anomalies in DJF, during El Niño and La Niña events.

shows the vertically integrated (1000 hPa to 300 hPa) water vapor flux (kg m^{-1} s^{-1}) and its divergence (kg m^{-2} s^{-1}). Anomalous southerly winds over southern China carried warm and wet air from the Bay of Bengal and the South China Sea and converged over PRD during the 2015 El Niño. The moisture flux was significantly strengthened and even transported to YRD in the 2018 El Niño, which is consistent with the wider range of precipitation anomalies in CP El Niño events than in EP El Niño events shown in Yu et al. (2020). Liu et al. (2020) also proposed that CP El Niño and Atlantic warming made an important contribution to the excessive amount of precipitation in winter 2018. The stronger moisture flux during El Niño increased the precipitation over PRD in 2015 and YRD in 2018 (Fig. 4(i–l)), which enhanced the wet deposition of $PM_{2.5}$ over these regions, while in the 2017 and 2020 La Niña events a reduction in precipitation was observed in southern China. The enhanced precipitation during the 2018 El Niño over YRD, together with the enhanced north-to-south $PM_{2.5}$ transport during the 2017 La Niña, explains the reduction in $PM_{2.5}$ concentration over YRD in 2018 relative to 2017 (Fig. 3(f)). Considering the comprehensive effects of winds and precipitation, the quantitative influences of ENSO on $PM_{2.5}$ over YRD should be analyzed case by case.

4. Summary

Based on observational $PM_{2.5}$ concentrations from September 2014 to August 2021, we investigated in this study the impacts of four ENSO events on wintertime near-surface $PM_{2.5}$ concentrations in China during 2014–2021. The wintertime $PM_{2.5}$ concentrations in BTH and FWP in the 2015 and 2018 El Niño were 28 μg m^{-3} and 19 μg m^{-3} higher than those in the 2017 and 2020 La Niña, respectively. This can partially be explained by the anomalous southerly (northerly) winds during El Niño (La Niña), resulting in the accumulation (diffusion) of $PM_{2.5}$ over BTH and FWP. The wintertime $PM_{2.5}$ concentrations in PRD in the 2015 and 2018 El Niño were 8 μg m^{-3} lower than those in the 2017 and 2020 La Niña owing to the enhanced water vapor flux and precipitation, leading to more $PM_{2.5}$ removal during El Niño events. In YRD, the enhanced precipitation in El Niño, especially in CP El Niño, favors the removal of $PM_{2.5}$ from the atmosphere, but the enhanced north-to-south $PM_{2.5}$ transport in El Niño favors an increase in $PM_{2.5}$ concentrations. The comprehensive effects of wind and precipitation anomalies lead to difficulties in accurately quantifying the impacts of ENSO on $PM_{2.5}$ over YRD, which should be analyzed case by case.

It should be noted that, with observational data alone, we did not specifically quantify the impacts of the changes in anthropogenic emissions in China in recent years, which could perturb the magnitude of the ENSO impacts on $PM_{2.5}$ concentrations illustrated in this study. Modeling studies are necessary for further analysis to distinguish the consequences on air pollutants caused by anthropogenic emissions and ENSO. In addition, due to the short history of $PM_{2.5}$ observations in China, only the $PM_{2.5}$ variations during four ENSO events were examined in this study. The impacts and mechanism can be further verified with more data in the near future.

Funding

This study was supported by the National Natural Science Foundation of China [grant number 41975159] and the National Key Research and Development Program of China [grant numbers 2020YFA0607803 and 2019YFA0606800].

Supplementary materials

Supplementary material associated with this article can be found, in the online version, at doi:10.1016/j.aosl.2022.100189.

References

Cai, W., Li, K., Liao, H., Wang, H., Wu, L., 2017. Weather conditions conducive to Beijing severe haze more frequent under climate change. Nat. Clim. Chang. 7 (4), 257–262. doi:10.1038/nclimate3249.

Chang, L., Xu, J., Tie, X., Wu, J., 2016. Impact of the 2015 El Nino event on winter air quality in China. Sci. Rep. 6, 34275. doi:10.1038/srep34275.

Cohen, A.J., Brauer, M., Burnett, R., Anderson, H.R., Frostad, J., Estep, K., Balakrishnan, K., et al., 2017. Estimates and 25-year trends of the global burden of disease attributable to ambient air pollution: an analysis of data from the global burden of diseases study 2015. Lancet 389 (10082), 1907–1918. doi:10.1016/S0140-6736(17)30505-6.

Ding, A.J., Huang, X., Nie, W., Sun, J.N., Kerminen, V.M., Petäjä, T., Su, H., et al., 2016. Enhanced haze pollution by black carbon in megacities in China. Geophys. Res. Lett. 43 (6), 2873–2879. doi:10.1002/2016GL067745.

Ding, Y., Liu, Y., 2014. Analysis of long-term variations of fog and haze in China in recent 50 years and their relations with atmospheric humidity. Sci. China Earth Sci. 57 (1), 36–46. doi:10.1007/s11430-013-4792-1.

Hersbach, H., Bell, B., Berrisford, P., Hirahara, S., Horányi, A., Muñoz-Sabater, J., Nicolas, J., et al., 2020. The ERA5 global reanalysis. Q. J. R. Meteorol. Soc. 146 (730), 1999–2049. doi:10.1002/qj.3803.

Huang, B., Thorne, P.W., Banzon, V.F., Boyer, T., Chepurin, G., Lawrimore, J.H., Menne, M.J., Smith, T.M., Vose, R.S., Zhang, H.M., 2017. Extended reconstructed sea surface temperature, version 5 (ERSSTv5): upgrades, validations, and intercomparisons. J. Clim. 30 (20), 8179–8205. doi:10.1175/JCLI-D-16-0836.1.

Gao, H., Li, X., 2015. Influences of El Nino Southern Oscillation events on haze frequency in eastern China during boreal winters. Int. J. Climatol. 35 (9), 2682–2688. doi:10.1002/joc.4133.

Liu, J., Wang, H., Lu, E., Kumar, A., 2019. Decadal modulation of East China winter precipitation by ENSO. Clim. Dyn. 52 (12), 7209–7223. doi:10.1007/s00382-016-3427-6.

Liu, Y., Hu, Z.Z., Wu, R., 2020. Was the extremely wet winter of 2018/2019 in the lower reach of the Yangtze River driven by El Niño–Southern Oscillation? Int. J. Climatol. 40 (15), 6441–6457. doi:10.1002/joc.6591.

Sun, J., Li, H., Zhang, W., Li, T., Zhao, W., Zuo, Z., Guo, S., Wu, D., Fan, S., 2018. Modulation of the ENSO on winter aerosol pollution in the eastern region of China. J. Geophys. Res. Atmos. 123 (21), 11–952. doi:10.1029/2018JD028534.

Wang, H.J., Chen, H.P., Liu, J., 2015. Arctic sea ice decline intensified haze pollution in eastern China. Atmos. Ocean. Sci. Lett. 8 (1), 1–9. doi:10.3878/AOSL20140081.

Wang, J., Liu, Y., Ding, Y., 2020. On the connection between interannual variations of winter haze frequency over Beijing and different ENSO flavors. Sci. Total Environ. 740, 140109. doi:10.1016/j.scitotenv.2020.140109.

Wang, X., Zhong, S., Bian, X., Yu, L., 2019. Impact of 2015–2016 El Niño and 2017–2018 La Niña on PM2.5 concentrations across China. Atmos. Environ. 208, 61–73. doi:10.1016/j.atmosenv.2019.03.035.

Xie, P., Arkin, P.A., 1997. Global precipitation: A 17-year monthly analysis based on gauge observations, satellite estimates, and numerical model outputs. Bull. Am. Meteorol. Soc. 78 (11), 2539–2558. doi:10.1175/1520-0477(1997)078<2539:GPAYMA>2.0.CO;2.

Yang, Y., Liao, H., Lou, S., 2016. Increase in winter haze over eastern China in recent decades: Roles of variations in meteorological parameters and anthropogenic emissions. J. Geophys. Res. Atmos. 121, 13050–13065. doi:10.1002/2016jd025136.

Yang, Y., Wang, H., Smith, S.J., Zhang, R., Lou, S., Qian, Y., Ma, P.-L., Rasch, P.J., 2018. Recent intensification of winter haze in China linked to foreign emissions and meteorology. Sci. Rep. 8, 2107. doi:10.1038/s41598-018-20437-7.

Yin, Z., Zhou, B., Chen, H., Li, Y., 2021. Synergetic impacts of precursory climate drivers on interannual-decadal variations in haze pollution in North China: A review. Sci. Total Environ. 755, 143017. doi:10.1016/j.scitotenv.2020.143017.

Yu, X., Wang, Z., Zhang, H., Zhao, S., 2019. Impacts of different types and intensities of El Niño events on winter aerosols over China. Sci. Total Environ. 655, 766–780. doi:10.1016/j.scitotenv.2018.11.090.

Yu, X., Wang, Z., Zhang, H., He, J., Li, Y., 2020. Contrasting impacts of two types of El Niño events on winter haze days in China's Jing-Jin-Ji region. Atmos. Chem. Phys. 20 (17), 10279–10293. doi:10.5194/acp-20-10279-2020.

Zeng, L., Yang, Y., Wang, H., Wang, J., Li, J., Ren, L., Li, H., Zhou, Y., Wang, P., Liao, H., 2021. Intensified modulation of winter aerosol pollution in China by El Niño with short duration. Atmos. Chem. Phys. 21 (13), 10745–10761. doi:10.5194/acp-21-10745-2021.

Zhang, G., Gao, Y., Cai, W., Leung, L.R., Wang, S., Zhao, B., Wang, M., Shan, H., Yao, X., Gao, H., 2019. Seesaw haze pollution in North China modulated by the subseasonal variability of atmospheric circulation. Atmos. Chem. Phys. 19 (1), 565–576. doi:10.5194/acp-19-565-2019.

Zhao, S., Li, J., Sun, C., 2016. Decadal variability in the occurrence of wintertime haze in central eastern China tied to the Pacific Decadal Oscillation. Sci. Rep. 6 (1), 1–9. doi:10.1038/srep27424.

Zhao, S., Zhang, H., Xie, B., 2018. The effects of El Niño–Southern Oscillation on the winter haze pollution of China. Atmos. Chem. Phys. 18 (3), 1863–1877. doi:10.5194/acp-18-1863-2018.

Zhao, W., Chen, S., Zhang, H., Wang, J., Chen, W., Wu, R., Xing, W., et al., 2022. Distinct Impacts of ENSO on Haze Pollution in the Beijing–Tianjin–Hebei Region between Early and Late Winters. J. Clim. 35 (2), 687–704. doi:10.1175/JCLI-D-21-0459.1.

Zou, Y., Wang, Y., Xie, Z., Wang, H., Rasch, P.J., 2020. Atmospheric teleconnection processes linking winter air stagnation and haze extremes in China with regional Arctic sea ice decline. Atmos. Chem. Phys. 20 (8), 4999–5017. doi:10.5194/acp-20-4999-2020.